GSC Advanced Research and Reviews
eISSN: 2582-4597 CODEN (USA): GARRC2
Cross Ref DOI: 10.30574/gscarr
Journal homepage: https://gscarr.gsconlinepress.com/

(RESEARCH ARTICLE)

Check for updates

ESTIMATING DAILY SOLAR IRRADIATION FROM SUNSHINE DURATION ACROSS THE SAHARA–SAHEL GRADIENT OF NIGER: AN ÅNGSTRÖM–PRESCOTT SCENARIO ASSESSMENT

Moumouni Guero Mohamed [1, 2, *]

[1] Department of Mechanical and Energy Engineering, POLYTECH Maradi, Dan Dicko Dankoulodo University of Maradi, BP 465, Maradi, Niger.
[2] Innovatech Smart Energies, Consulting and Expertise Firm, Maradi, Niger.
* Corresponding Author

ORCID Details
Moumouni Guero Mohamed; ORCID: 0000-0002-4183-8972.

GSC Advanced Research and Reviews, 2026, 29(01), 239–246

Publication history: Received on 07 September 2026; revised on 17 October 2026; accepted on 19 October 2026

Article DOI: https://doi.org/10.30574/gscarr.2026.29.1.0279

Copyright © 2026 Author(s) retain the copyright of this article. This article is published under the terms of the Creative Commons Attribution License 4.0

ABSTRACT

Ground-based irradiance measurements are almost absent in Niger, so photovoltaic (PV) planning relies on satellite or reanalysis products or on sunshine-duration proxies. This study estimates daily global horizontal irradiation (R_s) from ten years (2015–2024) of daily sunshine-duration records at three synoptic stations spanning the Sahara–Sahel gradient (Bilma, Agadez Aéro and N'Guigmi), using the Ångström–Prescott model applied at daily resolution with generic coefficients (a = 0.25, b = 0.50). A documented quality-control pass resolved duplicated monthly records, excluded values entered under non-existent dates and capped five marginal cases in which sunshine duration exceeded the astronomical day length. Coefficient uncertainty was represented by a scenario envelope (a = 0.20–0.30, b = 0.40–0.60) rather than a statistical interval. The central annual mean R_s was 5.57, 5.99 and 6.03 kWh m^{-2} d^{-1} at Agadez, Bilma and N'Guigmi, respectively. Monthly climatological means ranged from 4.64 to 6.61 kWh m^{-2} d^{-1}, whereas the coefficient scenarios shifted the annual means between 4.46 and 7.24 kWh m^{-2} d^{-1}. The June–August minimum of sunshine fraction was negatively associated with maximum relative humidity at Agadez (r = −0.53) and N'Guigmi (r = −0.69) but not at Bilma (r = +0.20), suggesting a different control at the Saharan station. The clearness index is shown to be an algebraic rescaling of the same input and is reported only as a diagnostic. The estimates are internally consistent but uncalibrated and unvalidated; a validation protocol against satellite and reanalysis products is specified.

Keywords: Solar irradiation; Sunshine duration; Ångström–Prescott model; Photovoltaic resource; Sahel; Niger

1 INTRODUCTION

Photovoltaic generation is widely regarded as one of the most promising options for expanding electricity access in the Sahel, and PV and hybrid mini-grids are increasingly being designed for rural electrification in Niger [1, 2]. Almost every statement about the solar resource of the country, however, comes from satellite or model products rather than from ground instruments: the country profile of the International Renewable Energy Agency (IRENA), for example, expresses

the national solar potential as PV yield classes derived from global atlas products [3]. The synoptic network of Niger records daily sunshine duration with Campbell–Stokes heliographs, which register sunshine when the direct irradiance exceeds 120 W m^{-2} [4], but it does not operate pyranometers, so no continuous ground record of irradiance exists against which satellite products or proxy models can be checked locally.

Where only sunshine duration is available, the Ångström–Prescott model is the standard way of estimating global irradiation from the fraction of possible sunshine hours [5, 6]. Its coefficients vary with climate, aerosol load and latitude, and are ideally calibrated against local pyranometer data [7–9]. In the absence of such data, generic coefficients can still provide a transparent first estimate, provided that the sensitivity to the coefficients is quantified and the result is eventually benchmarked against independent products such as NASA POWER [10], ERA5-Land [11] or the Copernicus Atmosphere Monitoring Service (CAMS) radiation service based on Heliosat-4 [12], following established validation practice [13].

The objectives of this study are (i) to estimate daily global horizontal irradiation at three synoptic stations spanning the Sahara–Sahel gradient of Niger from a documented, quality-controlled sunshine-duration record; (ii) to separate the seasonal (climatological) variability of the estimates from their sensitivity to the Ångström–Prescott coefficients; (iii) to test whether the summer minimum of sunshine fraction tracks atmospheric moisture at each station; (iv) to clarify the status of the clearness index, which is often presented as an independent check; and (v) to specify the validation that these estimates require before they can support PV design.

2 MATERIALS AND METHODS

2.1 Study area and data

The three stations lie along a roughly north–south transect through Niger (Table 1): Bilma in the hyper-arid central Sahara, Agadez Aéro at the Sahara–Sahel transition and N'Guigmi in the Sahelian Lake Chad basin. Daily sunshine duration (n, hours) and daily maximum relative humidity (RH_{max}, %) for 1 January 2015 to 31 December 2024 were provided by the Direction de la Météorologie Nationale (DMN) of Niger. No shortwave irradiance, diffuse fraction or aerosol optical depth measurement is available for any of the three stations.

Table 1: Station locations and climatic zones used in the solar-geometry calculation

Station	Latitude	Longitude	Elevation (m)	Climatic zone
Bilma	18.69°N	12.92°E	357	Hyper-arid Sahara
Agadez Aéro	16.97°N	7.98°E	502	Sahara–Sahel transition
N'Guigmi	14.25°N	13.12°E	286	Sahel / Lake Chad basin

2.2 Quality control

Table 2: Quality-control accounting for the daily sunshine-duration record, 2015–2024

Station	Calendar days	Valid days	Missing days (%)[a]	Duplicated station-months[b]	Marginal $n > N$ (capped)
Agadez Aéro	3,653	3,331	322 (8.8)	4 (2 conflicting)	2
Bilma	3,653	3,586	67 (1.8)	0	1
N'Guigmi	3,653	3,525	128 (3.5)	0	2

[a]Includes whole months absent from the source workbook: 212 days (7 months) at Agadez, 62 days (2 months) at Bilma and 123 days (4 months) at N'Guigmi.; [b]Conflicting duplicates were resolved as described in Section 2.2.

The source workbook stores one row per station and month. Four station-months were entered twice at Agadez (January 2019, October 2021, February 2022 and March 2022). Two duplicates were identical and were merged. The other two disagreed on a single day each: on 5 March 2022 one row gives 40.3 h, which exceeds the possible day length (11.7 h) by a factor of about 3.4, whereas the duplicate row gives 10.3 h, so the physically possible value was retained; on 12 January 2019 the two rows give 1.7 h and 10.7 h, both physically possible, so that day was set to missing. Five values entered under the non-existent dates of 29 February 2017 and 29 February 2021 were discarded. Every daily value exceeding the astronomically possible day length N (Eq. 5) was then flagged: five such cases remained, all marginal

(0.07 to 1.05 h above N), consistent with the 0.1 h reporting resolution of the heliograph record; they were retained with the sunshine fraction n/N capped at 1.0. Table 2 summarizes the resulting record.

2.3 Solar geometry

For each station and day of year J, the solar declination δ (rad), the inverse relative Earth–Sun distance d_r, the sunset hour angle ω_s (rad), the extraterrestrial irradiation on a horizontal surface R_a and the astronomically possible sunshine duration N (h) were computed with the FAO-56 formulation [5]:

$$\delta = 0.409 \sin\left(2\pi \frac{J}{365} - 1.39\right) \quad (1)$$

$$d_r = 1 + 0.033 \cos\left(2\pi \frac{J}{365}\right) \quad (2)$$

$$\omega_s = \arccos(-\tan\varphi \tan\delta) \quad (3)$$

$$R_a = \frac{24 \times 60}{\pi} G_{sc} d_r [\omega_s \sin\varphi \sin\delta + \cos\varphi \cos\delta \sin\omega_s] \quad (4)$$

$$N = \frac{24}{\pi} \omega_s \quad (5)$$

where φ is the station latitude (rad) and G_{sc} = 0.0820 MJ m^{-2} min^{-1} is the solar constant. With this constant, Eq. (4) gives R_a in MJ m^{-2} d^{-1}, which was converted to kWh m^{-2} d^{-1} by dividing by 3.6.

2.4 Ångström–Prescott model and coefficient scenarios

Daily global horizontal irradiation R_s was estimated for every valid day with the Ångström–Prescott model:

$$R_s = R_a \left(a + b \frac{n}{N}\right) \quad (6)$$

where n is the recorded sunshine duration (h) and a and b are empirical coefficients. The generic values a = 0.25 and b = 0.50 recommended when no local calibration exists [5] were used as the central estimate. The model was applied at daily resolution throughout, and every monthly or annual figure in this paper is an average of the same daily estimates. Because no pyranometer record exists for local calibration, the sensitivity to the coefficients was represented by two scenarios spanning values commonly reported for arid and semi-arid sites [7–9]: a low scenario (a = 0.20, b = 0.40) and a high scenario (a = 0.30, b = 0.60). The resulting range is a scenario envelope, not a statistical confidence interval.

2.5 Clearness index

The clearness index $k_T = R_s/R_a$ [14] is sometimes used as an independent check of Ångström–Prescott estimates. Substituting Eq. (6) gives

$$k_T = \frac{R_s}{R_a} = a + b \frac{n}{N} \quad (7)$$

which is an exact linear rescaling of the sunshine fraction already used to compute R_s. The clearness index is therefore reported only as a diagnostic and is not used as evidence that the estimates are correct. Its common use to estimate the diffuse fraction through empirical correlations [15] was not pursued, since no diffuse measurement is available to check such a split.

2.6 Association between sunshine fraction and humidity

To test the hypothesis that the summer minimum of sunshine fraction reflects monsoon moisture and cloudiness, the monthly climatological means of n/N were compared with those of RH_{max} at each station using the Pearson correlation coefficient r. Because only twelve monthly means are available per station, and because both variables share a strong seasonal cycle, these coefficients are reported as descriptive measures of association rather than as formal significance tests.

2.7 Software and data availability

All calculations were implemented in Python 3.11 with pandas [16] and NumPy [17], and figures were produced with Matplotlib [18]. The daily record, the quality-control log (including the resolution of each duplicated or flagged value) and the calculation scripts are available from the corresponding author on reasonable request.

3 RESULTS AND DISCUSSION

3.1 Seasonal cycle of estimated irradiation

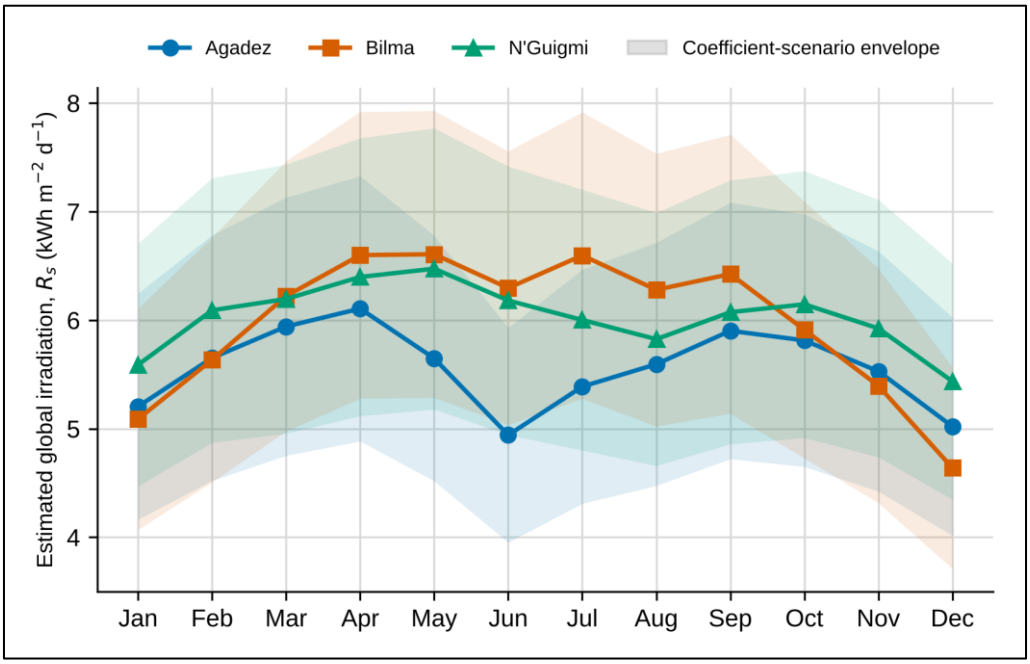


Figure 1: Climatological monthly mean of daily estimated global horizontal irradiation R_s at each station, 2015–2024. Lines: central Ångström–Prescott estimate (a = 0.25, b = 0.50); shaded bands: coefficient-scenario envelope (low: a = 0.20, b = 0.40; high: a = 0.30, b = 0.60).

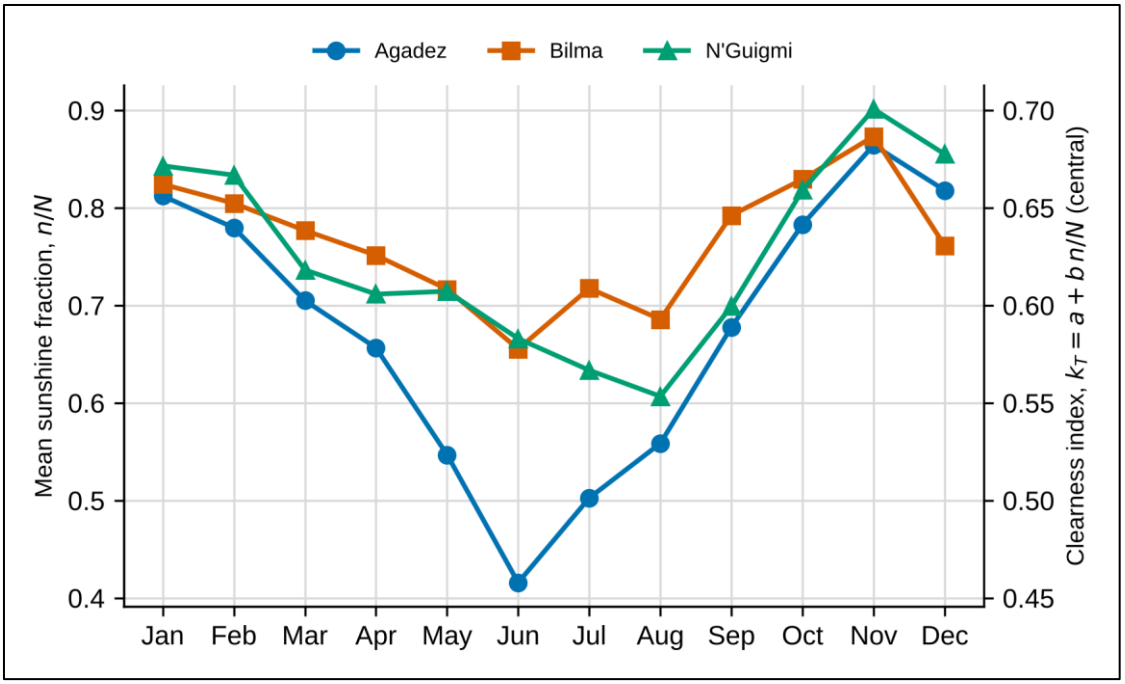


Figure 2: Climatological monthly mean sunshine fraction n/N at each station, 2015–2024. The right axis gives the corresponding clearness index under the central coefficients, k_T = 0.25 + 0.50 n/N, which is a linear rescaling of the same quantity (Section 2.5), not an independent result.

Fig. 1 shows the climatological monthly means of the central estimate with the coefficient-scenario envelope, and Fig. 2 the underlying sunshine fraction. Agadez and N'Guigmi show a primary maximum in April–May and a secondary maximum in September–October, separated by a summer minimum that is deepest at Agadez, where the mean sunshine

fraction falls to 0.42 in June. Bilma, the station furthest from the northward reach of the monsoon, has a much shallower summer dip and retains high irradiation from April to September, and its lowest monthly mean occurs in December, when the extraterrestrial irradiation is smallest.

3.2 Summer minimum of sunshine fraction and atmospheric moisture

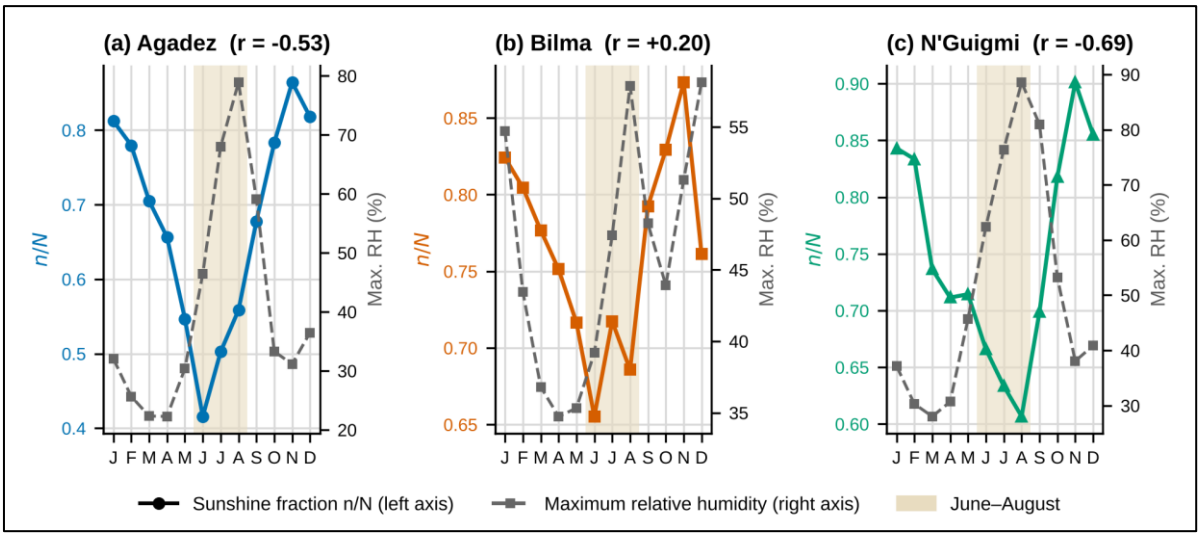


Figure 3: Climatological monthly sunshine fraction *n*/*N* (coloured, left axis) and maximum relative humidity (grey dashed, right axis) at (a) Agadez, (b) Bilma and (c) N'Guigmi, 2015–2024. The shaded band marks June–August; *r* is the Pearson correlation between the twelve monthly means. Each panel has its own axis ranges.

Fig. 3 compares the monthly sunshine fraction with the maximum relative humidity recorded at the same station. The association is negative and moderate at Agadez (r = -0.53) and stronger at N'Guigmi (r = -0.69), consistent with the attribution of the summer minimum to monsoon moisture and cloudiness. At N'Guigmi this agrees with the opposite loadings of insolation and relative humidity on the first principal component of the 2010–2019 meteorological record of the same station [19]. At Agadez, the sunshine minimum (June) precedes the humidity maximum (August) by two months, which suggests that pre-monsoon dust events may also contribute. At Bilma the association is weak and slightly positive (r = +0.20): the summer reduction is smaller (mean n/N of 0.686 in June–August against 0.792 in the other months) and is not captured by a humidity proxy, which points to a different control in the hyper-arid interior, such as the seasonal cycle of dust loading [20]. These station-specific associations are descriptive and should not be read as confirmed causal mechanisms.

3.3 Harmonized irradiation estimates

Table 3 gives every irradiation figure used in this paper from a single calculation. Two different ranges must be distinguished: the climatological range describes how the central monthly mean varies through the year, whereas the coefficient-scenario range describes how the annual mean itself shifts under the low and high coefficient scenarios. Pooled across the three stations, the first spans 4.64 to 6.61 kWh m^{-2} d^{-1} and the second 4.46 to 7.24 kWh m^{-2} d^{-1}; the two should not be combined into a single uncertainty statement. The coefficient choice therefore moves the annual mean by about ±20%, which is larger than the difference between stations, so the generic coefficients, rather than the sunshine record, dominate the uncertainty of the absolute values.

Table 3: Harmonized Ångström–Prescott irradiation estimates, 2015–2024 (kWh m^{-2} d^{-1})

Station	Valid days	Annual mean R_s, central estimate	Climatological range of monthly means[a]	Coefficient-scenario range of annual mean[b]
Agadez Aéro	3,331	5.57	4.94–6.11	4.46–6.69
Bilma	3,586	5.99	4.64–6.61	4.80–7.19
N'Guigmi	3,525	6.03	5.44–6.47	4.83–7.24

[a]Central coefficients (a = 0.25, b = 0.50).; [b]Low (a = 0.20, b = 0.40) and high (a = 0.30, b = 0.60) coefficient scenarios.

3.4 What the estimates represent

Three physically distinct quantities are often discussed together in the literature on dust and solar energy in the Sahara–Sahel region: global horizontal irradiation at the surface, which is what Table 3 reports; atmospheric transmission losses caused by dust, aerosols and clouds; and PV soiling losses caused by dust deposited on the module surface [21, 22]. The sunshine-based model captures atmospheric attenuation only indirectly, because a hazy day can still register heliograph sunshine while diffuse and total irradiation are reduced [20]. Soiling is a separate process at the module surface; large PV output reductions reported for dusty conditions refer to system output, not to surface irradiation, and the estimates in Table 3 should neither be rescaled by such figures nor be assumed to include them. There is also no basis in this dataset for asserting that the estimates are an upper or a lower bound of the true resource.

3.5 Validation required before use

No independent validation of the estimates was performed in this study, and this is its most important limitation. A locally meaningful validation would compare the daily estimates, at the coordinates of each station, with an independent satellite or reanalysis product (NASA POWER [10], ERA5-Land [11] or CAMS [12]; such products are widely used for solar-resource assessment in West Africa [23]), using the mean bias error, the mean absolute error, the root-mean-square error and the correlation coefficient [13], computed by station, month and season, and with part of the record held out to test whether any bias correction generalizes. Without such an external benchmark, internal consistency cannot distinguish an accurate estimate from a consistently biased one.

3.6 Limitations

Uncalibrated coefficients. The coefficients are generic values; the scenario envelope communicates the resulting sensitivity but is not a substitute for calibration against measured irradiation. Daily resolution. The model estimates daily totals and says nothing about the sub-daily distribution of irradiance that matters for inverter sizing, storage and intermittency. Loss mechanisms. Estimates for PV yield will require a separate, local assessment of soiling and system losses (Section 3.4). Small samples for the humidity test. The correlations of Section 3.2 rest on twelve climatological means per station. Data gaps. Whole months are missing at each station (Table 2), most at Agadez, so the monthly climatologies of the affected months rest on fewer years.

4 CONCLUSION

A documented quality-control pass and a single daily Ångström–Prescott calculation provide internally consistent estimates of daily global horizontal irradiation at three synoptic stations of Niger for 2015–2024. The central annual means lie between about 5.6 and 6.0 kWh m^{-2} d^{-1}, with a station-dependent seasonal cycle: a deep summer minimum at Agadez, a moderate one at N'Guigmi and only a shallow one at Bilma. The summer reduction of sunshine fraction is associated with humidity at the two Sahelian-margin stations but not at Bilma. The choice of coefficients shifts the annual means by about ±20%, more than the differences between stations, and the clearness index adds no independent information. These results are an exploratory regional characterization; calibration against measured irradiation, or at least validation against independent satellite and reanalysis products following the protocol of Section 3.5, is required before they are used for PV design or investment decisions.

STATEMENTS ON COMPLIANCE WITH ETHICAL STANDARDS

Acknowledgments

The author thanks the Direction de la Météorologie Nationale (DMN) of Niger for providing the meteorological records. This research received no specific grant from any funding agency in the public, commercial or not-for-profit sectors. Disclosure of the use of generative artificial intelligence: Claude (Anthropic; model claude-opus-5-5, accessed through claude.ai, October 2026) was used for language editing, for formatting the manuscript to the journal guidelines, for verification of bibliographic metadata. The author reviewed all outputs and takes full responsibility for the content.

Disclosure of conflict of interest

The author runs Innovatech Smart Energies (listed as a secondary affiliation), an engineering consultancy in the energy sector. The firm did not fund this study and had no role in its design, analysis, interpretation or writing. No other conflict of interest to be disclosed.

REFERENCES

[1] Moumouni Guero M, Prodjinonto V. Climate, environmental and dynamic performance assessment of a PV-wind-battery mini-grid in Tafaghatt, Niger. Int J Environ Clim Change. 2026;16(9):197–213. doi:10.9734/ijecc/2026/v16i95641

[2] Moumouni Guero M, Prodjinonto V. Technical design and optimal sizing of a photovoltaic-wind hybrid system for rural electrification: case study of Tafaghatt, Niger. Curr J Appl Sci Technol. 2026;45(9):75–86. doi:10.9734/cjast/2026/v45i94749

[3] International Renewable Energy Agency. Energy profile: Niger [Internet]. Abu Dhabi: IRENA; 2025 [cited 2026 Oct 14]. Available from: https://www.irena.org/-/media/Files/IRENA/Agency/Statistics/Statistical_Profiles/Africa/Niger_Africa_RE_SP.pdf

[4] World Meteorological Organization. Guide to meteorological instruments and methods of observation. WMO-No. 8, 2014 edition, updated in 2017. Geneva: WMO; 2017.

[5] Allen RG, Pereira LS, Raes D, Smith M. Crop evapotranspiration: guidelines for computing crop water requirements. FAO Irrigation and Drainage Paper 56. Rome: Food and Agriculture Organization of the United Nations; 1998.

[6] Duffie JA, Beckman WA. Solar engineering of thermal processes. 4th ed. Hoboken (NJ): Wiley; 2013. doi:10.1002/9781118671603

[7] Martínez-Lozano JA, Tena F, Onrubia JE, de la Rubia J. The historical evolution of the Ångström formula and its modifications: review and bibliography. Agric For Meteorol. 1984;33(2–3):109–28. doi:10.1016/0168-1923(84)90064-9

[8] Besharat F, Dehghan AA, Faghih AR. Empirical models for estimating global solar radiation: a review and case study. Renew Sustain Energy Rev. 2013;21:798–821. doi:10.1016/j.rser.2012.12.043

[9] Almorox J, Benito M, Hontoria C. Estimation of monthly Ångström–Prescott equation coefficients from measured daily data in Toledo, Spain. Renew Energy. 2005;30(6):931–6. doi:10.1016/j.renene.2004.08.002

[10] Sparks AH. nasapower: a NASA POWER global meteorology, surface solar energy and climatology data client for R. J Open Source Softw. 2018;3(30):1035. doi:10.21105/joss.01035

[11] Muñoz-Sabater J, Dutra E, Agustí-Panareda A, Albergel C, Arduini G, Balsamo G, et al. ERA5-Land: a state-of-the-art global reanalysis dataset for land applications. Earth Syst Sci Data. 2021;13(9):4349–83. doi:10.5194/essd-13-4349-2021

[12] Qu Z, Oumbe A, Blanc P, Espinar B, Gesell G, Gschwind B, et al. Fast radiative transfer parameterisation for assessing the surface solar irradiance: the Heliosat-4 method. Meteorol Z. 2017;26(1):33–57. doi:10.1127/metz/2016/0781

[13] Gueymard CA. A review of validation methodologies and statistical performance indicators for modeled solar radiation data: towards a better bankability of solar projects. Renew Sustain Energy Rev. 2014;39:1024–34. doi:10.1016/j.rser.2014.07.117

[14] Liu BYH, Jordan RC. The interrelationship and characteristic distribution of direct, diffuse and total solar radiation. Sol Energy. 1960;4(3):1–19. doi:10.1016/0038-092X(60)90062-1

[15] Erbs DG, Klein SA, Duffie JA. Estimation of the diffuse radiation fraction for hourly, daily and monthly-average global radiation. Sol Energy. 1982;28(4):293–302. doi:10.1016/0038-092X(82)90302-4

[16] McKinney W. Data structures for statistical computing in Python. In: van der Walt S, Millman J, editors. Proceedings of the 9th Python in Science Conference; 2010 Jun 28–Jul 3; Austin, TX. p. 56–61. doi:10.25080/Majora-92bf1922-00a

[17] Harris CR, Millman KJ, van der Walt SJ, Gommers R, Virtanen P, Cournapeau D, et al. Array programming with NumPy. Nature. 2020;585(7825):357–62. doi:10.1038/s41586-020-2649-2

[18] Hunter JD. Matplotlib: a 2D graphics environment. Comput Sci Eng. 2007;9(3):90–5. doi:10.1109/MCSE.2007.55

[19] Moumouni Guero M, Prodjinonto V, Fannou JLC. Correlation of meteorological parameters to characterize wind sites: a case study of N'Guigmi, Niger. Glob NEST J. 2022;24(2):337–43. doi:10.30955/gnj.004155

[20] Haywood J, Francis P, Osborne S, Glew M, Loeb N, Highwood E, et al. Radiative properties and direct radiative effect of Saharan dust measured by the C-130 aircraft during SHADE: 1. Solar spectrum. J Geophys Res. 2003;108(D18):8577. doi:10.1029/2002JD002687

[21] Sarver T, Al-Qaraghuli A, Kazmerski LL. A comprehensive review of the impact of dust on the use of solar energy: history, investigations, results, literature, and mitigation approaches. Renew Sustain Energy Rev. 2013;22:698–733. doi:10.1016/j.rser.2012.12.065

[22] Isaacs S, Kalashnikova O, Garay MJ, van Donkelaar A, Hammer MS, Lee H, et al. Dust soiling effects on decentralized solar in West Africa. Appl Energy. 2023;340:120993. doi:10.1016/j.apenergy.2023.120993

[23] Sterl S, Liersch S, Koch H, van Lipzig NPM, Thiery W. A new approach for assessing synergies of solar and wind power: implications for West Africa. Environ Res Lett. 2018;13(9):094009. doi:10.1088/1748-9326/aad8f6